An Assessment of the New LS-DYNA® Multi-Layered Solid Element: Basics, Patch Simulation and its Potential for Thick Composite Structural Analysis

Madhukar Chatiri[1], Thorsten Schütz[2], Anton Matzenmiller[3]

[1]*CADFEM GmbH, Grafing/Munich, Germany, mchatiri@cadfem.de*
[2]*Adam Opel GmbH, GM APC E, Mainz-Kastel, Germany, thorsten.schuetz@de.opel.com*
[3]*Dept. of Mech. Engineering, Univ. of Kassel, Kassel, Germany, post-structure@uni-kassel.de*

Abstract

Limitation of fossil fuels and global warming favor the introduction of new powertrain concepts for road vehicles with highest efficiency and low greenhouse gas emissions. Fuel cell vehicles offer the highest potential for sustainable mobility in the future. One major component of fuel cell vehicles is the hydrogen storage system. A promising and currently the most-used approach is to store hydrogen in wet-wound carbon fiber reinforced plastic (CFRP) vessels manufactured by a filament winding process with an operating pressure of up to 70 MPa (hereafter referred as H_2 vessel). Due to the inherent complexity and the 3-dimensional nature, accurate behavior of such thick composite structures in impact simulations needs an adequate representation of the composite plies.

Modeling thick composite structures with two-dimensional elements will produce inaccurate results in transverse normal direction. Therefore, 3D modeling should be used but the idealization of each ply with one solid element leads to undesirably large models and is impractical for large structures. Hence, representation of several plies in one solid element and more such elements across the thickness is aspired. An improved multi-layered solid element showing excellent efficiency of CPU time is implemented in the code of LS-DYNA® Version 971 R4. Like any brick element, it resolves the 3D stress state necessary for impact directions normal to the outer vessel surface. The element allows the definition of multiple integration points through the thickness in order to account for stacks of plies with arbitrary fiber orientation. By defining several layers with different material properties and ply orientations inside one multi-layered solid, the number of elements through the thickness is remarkably reduced and still, the result is close to the one obtained from the detailed finite element model of one brick element per layer. As depicted in Fig.1.2, a complex laminate configuration consisting of 18 different plies with varied fiber angles is represented by one multi-layered solid element with 18 integration points through the thickness.

The above new element formulation is presented in this paper describing simulation results for both, different patches and for thick composite structures such as for hydrogen storage H_2 vessels.

Keywords: *Multi-layered solid, filament winding, thick composites, H_2 pressure vessel analysis*

1 Basics and modeling of thick composites

1.1 Introduction

Compared to metallic fuel tanks, filament wound-pressure tanks have remarkable properties with respect to specific modulus, thermal resistance and endurance. However, modeling and analyzing such tank systems is rather complex for following reasons: In these high-pressure fuel tanks, the fiber orientation varies in both, longitudinal and thickness direction, also the wall thickness is in the range of 40 to 60 mm. To reduce the idealization effort of thick composite structures, they are modeled with two-dimensional elements, such as plates and shells. However, this will produce inaccurate results because structures are so thick that the plane stress condition is not applicable. Three-dimensional elements should be used in this case. But in three-dimensional modeling, it is impossible to account for all the layers and their different material properties with only one solid element through the thickness. Thus, a new layered solid element has been implemented in LS-DYNA® comprising several plies with varying fiber orientation and thickness in a single solid element – see [1].

In the present paper, the new layered solid element in LS-DYNA, its formulation, numerical patch tests and its potential for the analysis of thick composite structures are investigated.

1.2 Different ways of modeling thick composite laminates

Modeling of thick composite structures should not only involve the global structural behaviour but should also include the complete three-dimensional stress state. Traditionally different approaches have been used to model thick composite structures as shown in Fig.1.1.
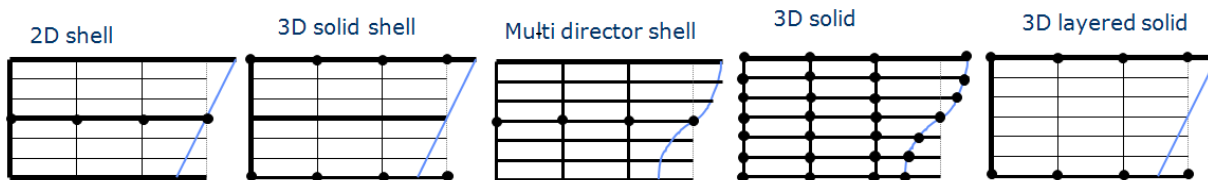

Fig. 1.1: Kinematic modeling of layered composite structure with different elements [8]

They can be modeled with shell elements wherein the normal stresses are neglected (which have 6 degrees of freedom, 3 translational and 3 rotational). Also, solid shell elements which have only displacement degrees of freedom have been used. In addition to the convenient inclusion of three-dimensional constitutive models, these elements provide a straightforward extension to geometrically non-linear problems, particularly in the presence of large rotations, since only translational degrees of freedom are involved. As a third advantage, modeling of transverse shear stresses is improved by introducing a director for each layer (multi-director formulation) [2]. An obvious discretization approach therefore is to use one solid element for each layer. However, this approach is not practical as it requires a too large computational effort. Apart from the above element modeling, different homogenization techniques used – like classical laminate theory giving smeared properties for the laminate. This approach helps to save numerical expenses and can be used to represent global structural behavior. But it cannot be used for the detailed 3D stress-strain analysis specifically with respect to the stress resolution in thickness direction.

The present paper focuses on the last approach, wherein the new multi-layered solid element can incorporate different material layers with varying fiber angles, variable thickness for the different layers inside the hexahedron and with multiple integration points through the thickness – see Fig. 1.2. By defining several layers with different material properties and ply orientations inside one layered solid, the number of elements through the thickness is remarkably reduced and still the result is close to the one obtained from the detailed finite element model of one brick element per layer.
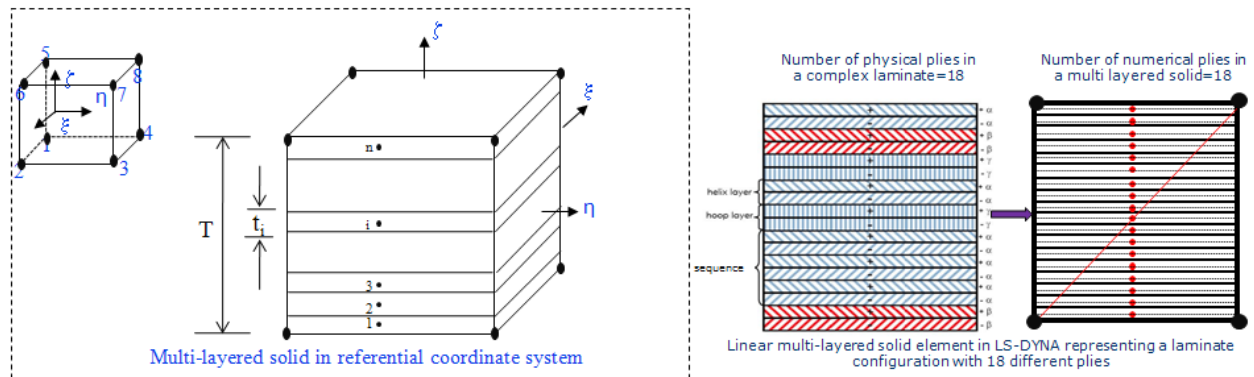

Fig. 1.2: Eight-node multi-layered solid element

2   Element formulation

2.1 Explicit eight-node layered solid element

The 8-node layered solid element in LS-DYNA, which can be accessed under thick shell element formulation 5, uses one integration point per layer and any number of integration points through the thickness – see Fig. 1.2. Like any brick element, it resolves the 3D stress state. Different material models may be assigned to each layer, using *PART_COMPOSITE or *INTEGRATION_SHELL cards. The tri-linear solid element is the starting point for the strain field, but enhanced assumptions about the strain field remove shear and volumetric locking. Also, a modification to the thickness strain is made for anisotropic materials and mixed materials to assure that the thickness stress is constant through the thickness. Also laminated shell theory [11] is applied to the transverse shear strain field to improve the transverse shear stress distribution through thickness and, hence, the need for the external shear correction factor is eliminated. Pursuant to these corrections, the improved multi- layered solid element behaves accurately when loaded either in plane stress or in three dimensional stress conditions. Zero energy modes that result from reduced integration in layer directions are eliminated by hourglass control derived from the type 6 one in LS-DYNA.

The formulation of type 6 hourglass control in LS-DYNA is based on ASQBI (assumed strain quintessential bending incompressible) hourglass control in Belytschko and Bindeman [1]. In equations (3.22) through (3.27) in the above referenced paper, it is demonstrated that the terms used to evaluate hourglass control can also be used to evaluate the strain at any point in the element domain. These formulae allow the strain tensor to be a measure at very low cost since the **B** matrix does not need to be evaluated for each integration point. It is possible to use the ASQBI strain fields with multiple integration points without encountering locking since this strain field maintains zero dilatation in the non-constant part of the strain field. For isotropic

materials with the same properties in each layer, this strain field is used directly with a 3D stress update routine. For anisotropic materials with principal directions that vary by layer, an additional correction is needed for the thickness strain term due to Poisson's effect which is directionally dependent and, therefore, varies by layer. Similarly, mixing materials in the layers requires a correction due to both Poisson's effects and a variation in stiffness.

The new multi-layered solid element requires hourglass control because it is not rank sufficient. ASQBI hourglass control is designed for brick elements that have 12 zero energy deformation modes. With more than one integration point through its thickness, 4 of these modes, two that correspond to bending and two that correspond to torsion, result in non-zero strains so that only 8 zero energy modes remain. Each of these modes can be identified as terms in ASQBI hourglass control and only the remaining 8 ones are used. In this way, the hourglass control is orthogonal to the strain fields in the element.

2.2 Element description in LS-DYNA

The new multi-layered solid element in LS-DYNA can be accessed under thick shell formulation 5 (tshell-elform = 5). The layered section can be defined with the *SECTION_TSHELL card in combination with the *INTEGRATION_SHELL or with *PART_COMPOSITE cards. Exemplarily, modeling a laminate with lay-up of $(+45/-45])_s$ configuration is shown in the appendix.

3   Numerical examples

A pragmatic approach is used to test the new layered solid element in LS-DYNA. Numerical testing is performed in three parts, consisting of one-element tests, composite benchmark tests as given in the literature, and component tests as performed for the Adam OPEL GmbH in Mainz-Kastel.

3.1 One-element examples

Initially the new layered solid element is verified with different one-element tests, i.e. with and without layered configurations. A test matrix is prepared which contains the new layered solid, shell and conventional solid elements with layer orientations for e.g. $(0)_4$, $(0/90)_s$, $(+45/-45)_s$ - see Fig. 3.2 - and for comparison also one without any preferred layer direction. The new layered solid element is tested with respect to tension, compression, shear and bending load cases both in longitudinal and transverse fiber direction. The results are compared with analytical solutions from structural mechanics as well as those from standard shell elements, and one-point hexahedrons in LS-DYNA.

3.1.1 Non-layered configuration tests

Firstly, the layered solid was verified with standard solid and shell elements without layered configurations. A hexahedron in the form of a regular 1mm x 1mm x 1mm cube for solid and layered solid elements, and a square plate of 1mm edge length and with a thickness of 1mm is used for the verification by means of the results from the shell element for the "one-element" tests. For all the simulation models the indices 1, 2, and 3 refer to principal material directions. The magnitude of the loading, applied by boundary conditions with uniformly prescribed

displacements is small enough and, thus, a linear elastic material response is assumed. The orthotropic elasticity model with damage i.e.*MAT_COMPOSITE_DAMAGE (*MAT_022) in LS-DYNA - is used for all the runs.

The material parameters of linear orthotropic elasticity for all one element tests are $E_{11} = 1.32$ x 10^5 N/mm^2, $E_{22} = E_{33} = 10\ 755$ N/mm^2, $\nu_{21} = \nu_{31} = 0.019$, $\nu_{23} = 0.490$, $G_{12} = G_{13} = 5\ 653$ N/mm^2, $G_{23} = 3378$ N/mm^2.

In the post processing, the internal strain energy density in Eq. 3.1, the energy ratio in Eq. 3.2, the reaction forces, and the stresses are checked with the analytical solution.

Internal strain energy
$$E_{internal} = \frac{1}{2} \int_V (C_{ij}\varepsilon_j)\varepsilon_i dv \qquad [3.1]$$

Energy ratio
$$e = \frac{E_{total}}{E_{kin}^0 + E_{internal}^0 + W_{external}} \qquad [3.2]$$

where the total energy E_{total} in each time step must be equal to the initial kinetic and internal energy E_{kin}^0, $E_{internal}^0$ plus the external work $W_{external}$ in order to exclude hourglassing of the underintegrated elements.

$$\underbrace{E_{kin} + E_{internal} + E_{rigidwall} + E_{hourglass} + E_{damping} + E_{sliding}}_{E_{total}} = E_{kin}^0 + E_{internal}^0 + W_{external}$$

Also, the result for the layered solid is compared to the standard hexahedron and the shell element simulations. Exemplarily shown are the results from the uniaxial tensile loading in x-direction - see Fig.3.1. Table 3.1 summarizes the results for the internal energy, the reaction forces, and the stress components. As seen from the table, the various results from the layered solid element are identical with the analytical reference solution for the shell and solid elements. Similar tests and comparisons are carried out for compression, bending and shear load cases.
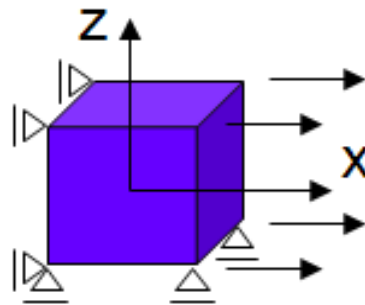

Fig.3.1: Uniaxial tensile test in the x- direction

component	analytical solution	solid type 1	shell type 2	layered solid tshell type 5
internal energy	26 N-mm	26 N-mm	26 N-mm	26 N-mm
reaction force	2.64kN	2.64kN	2.64kN	2.64kN
inplane stress (σ_x)	2640 MPa	2640 MPa	2640 MPa	2640 MPa

Table 3.1.: Results for uniaxial tensile test in x_1-direction

3.1.2 Layered configuration tests

The above mentioned tests are again performed with different fiber orientations (Fig. 3.2) and the results of the layered solid are compared to the layered shell element, where the in-plane components are verified. The lay-up of the laminate – i.e. ply thickness, ply orientation – as described previously, is defined by the input options *SECTION_TSHELL for the layered solid, *SECTION_SHELL for the shell element and the *INTEGRATION_SHELL card in the input.
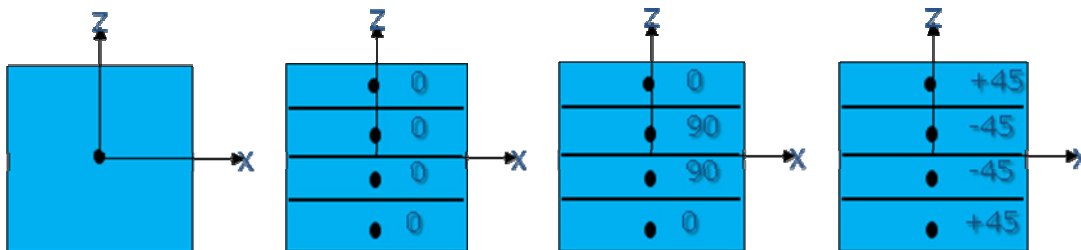
Fig.3.2.: Laminate configurations for one-element test

As an example the results are given from the uniaxial tensile load case on [0-0]$_s$, [0-90]$_s$ and [+45-45]$_s$ laminate configurations in x-direction – see Table 3.2. The in-plane stress component σ_x in the layer coordinate system for the new solid element is verified by means of the analytical and the layered shell element solution. The results of the layered hexahedron are in excellent agreement with the laminate shell element.

laminate configuration	analytical solution	shell type 2	layered solid tshell type 5
(0)$_4$	2640 MPa	2640 MPa	2640 MPa
(0/90)$_S$	2640 MPa	2640 MPa	2640 MPa
(45/-45)$_S$	355 MPa	355 MPa	355 MPa

Table 3.2: Comparison of in-plane stress σ_x in layer co-ordinate system

3.1.3 Element tests in thickness direction for layered configuration

In order to verify the thickness stress and strain components of the layered solid element, hexahedrons are stacked on top of each other in order to compare their solution to the results of a single layered solid element – see Figs. 3.3 and 3.4. Uniaxial compression in thickness (z) direction is applied to the single-layered solid element as well as to the four-stacked hexahedrons. The layer configuration is (0/90)$_S$ in both cases. One-point integration is used for the standard hexahedrons in the stack and also for each lamina in the new LS-DYNA layered solid. For this, the option *ELEMENT_SOLID_ORTHO is used in LS-DYNA.

Laminate configuration of 0-90-90-0 defined by 4 solid hexahedrons with *element_solid_ortho option

Laminate configuration of 0-90-90-0 defined by 1 layered solid element with 4 integration points across the thickness
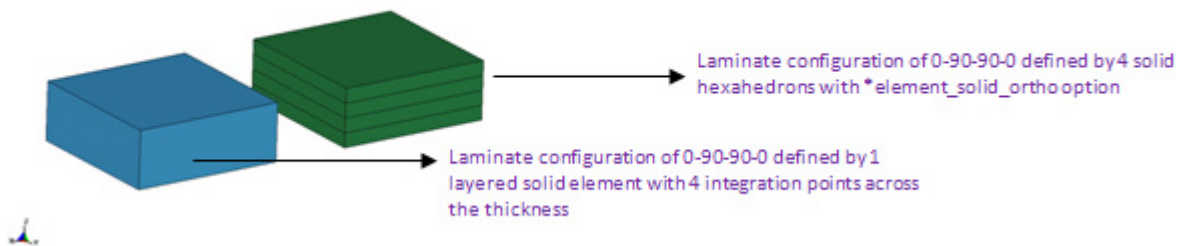
Fig.3.3: Layered solid and stacked one-point solid

The force-displacement curve of the layered solid element and the one of the four hexahedrons are plotted in Fig. 3.5. As they coincide, the through-the-thickness modeling approach in LS-DYNA may be considered as verified.
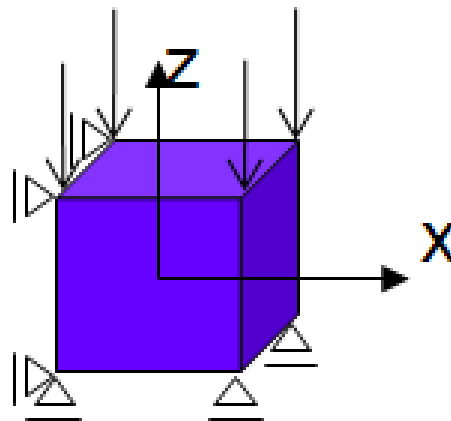

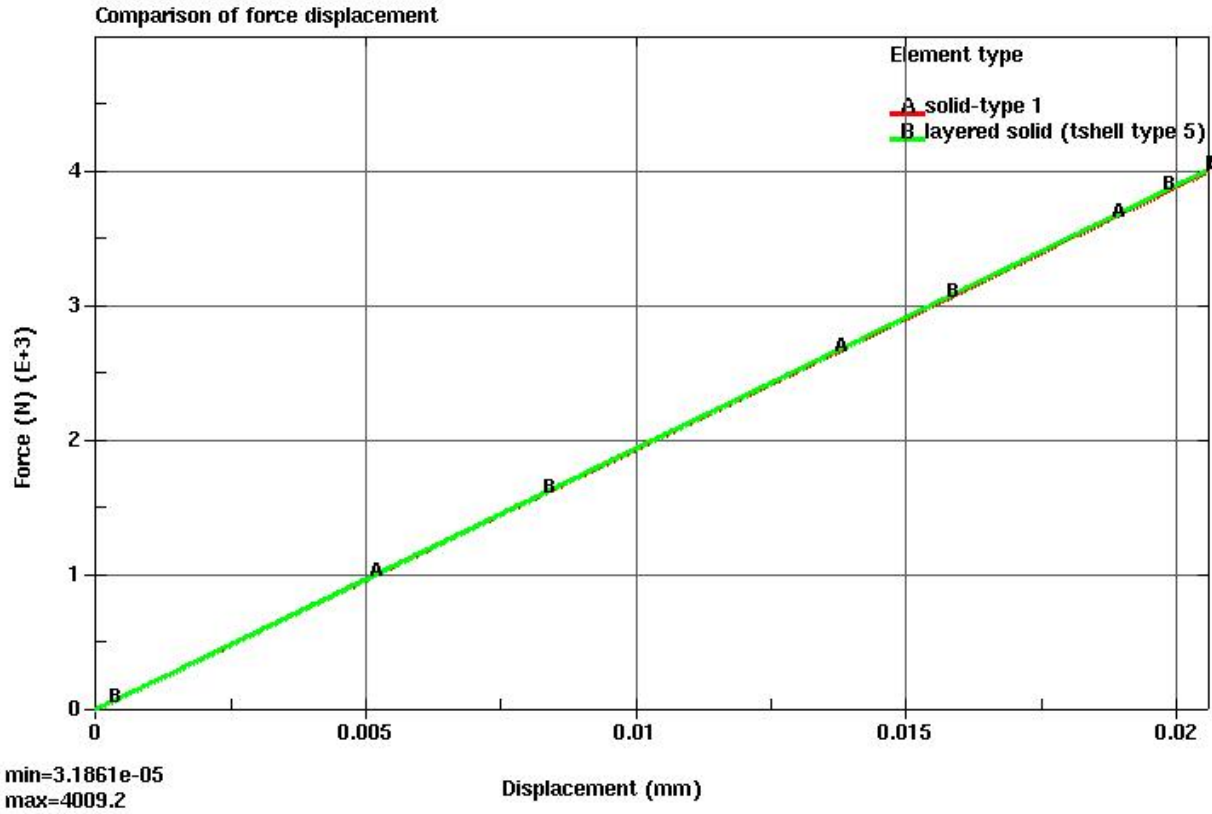Fig. 3.4.: Uniaxial compression test in the thickness z-direction

Fig. 3.5.: Comparison of force-displacement curves for solid and layered solid elements

As previously discussed about the constant thickness stresses for the layered solid element, Fig. 3.6 depicts that the thickness stress (σ_{33}) is constant across the thickness in all the laminae $(0/90)_S$ inside the layered solid element. Also, the thickness stresses are in excellent agreement with the result of the stacked hexahedron model.
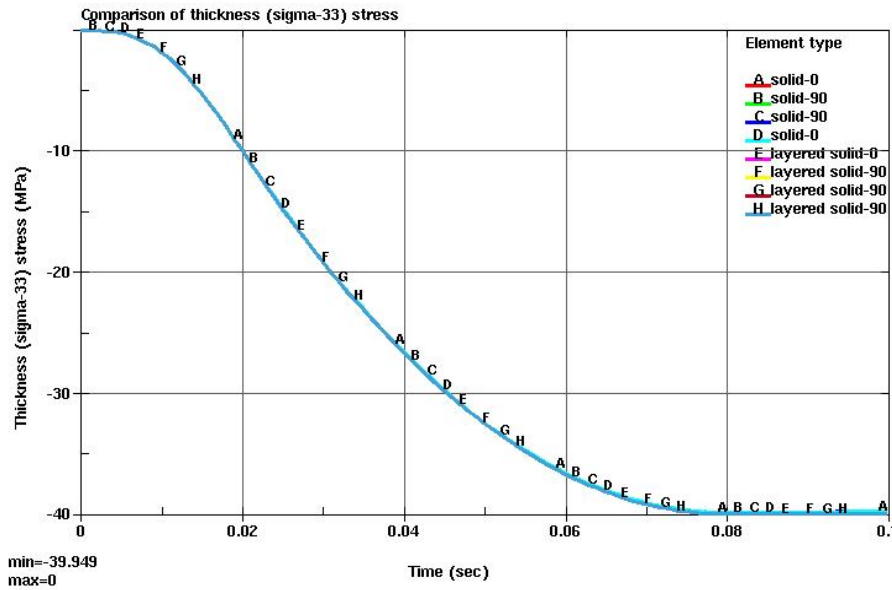

Fig. 3.6: Comparison of thickness (σ_{33}) stresses in individual stacked solid elements and different layers of layered solid elements.

3.2 Cantilever beam

After the one-element tests, the layered solid element is investigated at various composite benchmark examples from the literature. Fig 3.7 shows a linear elastic cantilever beam with a point load at its end.
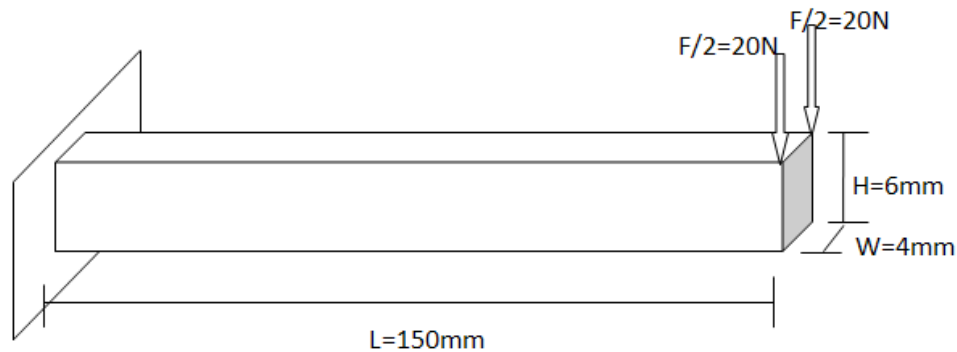

Fig. 3.7: Problem description for cantilever beam subjected to point load

Orthotropic material parameters for the cantilever test are E_{11} = 146.9 GPa, E_{22} = E_{33} = 10.9 GPa, v_{21} = v_{31} = 0.028, v_{23} = 0.776, G_{12} = G_{13} = 10.89 GPa, G_{23} = 6.4 GPa.

The above cantilever bending problem was simulated with two models. The first one was to check bending behavior of a normal orthotropic material without layer configuration and the second one with 0-90-90-0 layer configuration. According to the structural mechanics, deflection at the end of the beam would be w = FL^3/3EI = 4.25 mm. But this equation cannot be used for comparison here because of orthotropic material. With the convergence studies it was possible to get a converged solution of 4.30 mm.

The second model was simulated with one layered solid element across thickness with 0-90-90-0 configuration and the displacement achieved was 5.01 mm. Note, the converged displacement solution in reference [7] is 4.83 mm.

3.3 Verification of transverse stresses inside multi-layered solid

3.3.1 Cantilever beam under pressure loading

The cantilever beam of Fig. 3.8 is modeled with 5 multi-layered solid elements each with 5 integration points in thickness direction, 20 elements in the length direction and 5 elements in the width direction. With increasing number of elements through the thickness (see Fig. 3.9), the multi-layered solid approximates the analytical solution [3] for transverse normal stresses. The analytical solution for transverse normal stresses is given by

$$\sigma_{33} = -\frac{q}{2} + q\left[\frac{1}{4}\left(\frac{z}{h}\right)^3 - \left(\frac{3z}{4h}\right)\right]$$ [3.3]
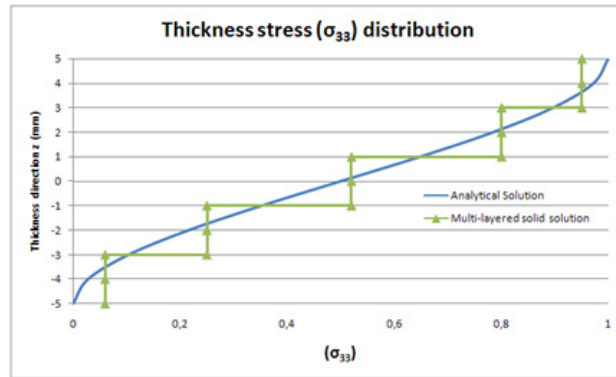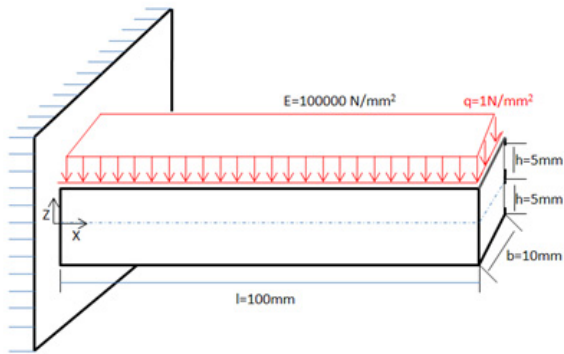
Fig.3.8: Problem description for cantilever beam subjected to pressure loading

Fig.3.9: Distribution of thickness stress for $\nu=0.0$ and 5 multi-layered solid elements through thickness

3.3.2 Cantilever beam under end load

The cantilever beam of Fig. 3.10 is modeled with 1 multi-layered solid element with 10 integration points in thickness direction, 20 elements in the length direction and 1 element in the width direction. With increasing number of IPs through the thickness (see Fig. 3.11), the multi-layered solid element approximates the analytical solution [3] for transverse shear stresses. The analytical solution for transverse shear stresses is given by

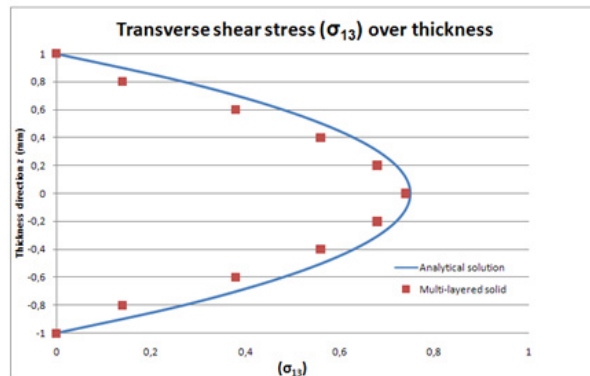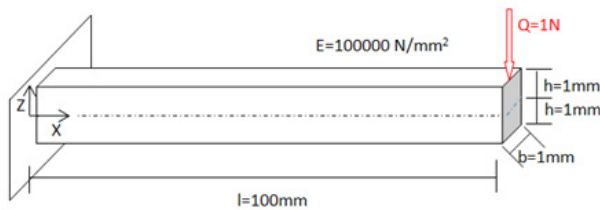$$\sigma_{13} = \frac{3Q}{4b} + \left[1 - \left(\frac{z}{h} \right)^2 \right] \qquad\qquad [3.4]$$

Fig. 3.10.: Problem description for cantilever beam subjected to point loading

Fig. 3.11.: Distribution of σ_{13} for $\nu=0.0$ and 1 multi-layered solid element through thickness

3.4 Thick walled cylinder under internal pressure

Consider a thick cylinder of inside radius r_i and outside radius r_o subjected to an internal pressure p_0. The finite element model of the radial symmetric field problem consists of a circular segment discretized with variable number of multi-layered solid elements in radial direction (see Fig.3.12). The problem is subjected to plane strain conditions. With increasing number of

elements in the radial direction, the multi-layered solid approximates the analytical solution [12] for radial and hoop stresses. The analytical solution for the distribution of radial and hoop stresses through the thickness of the tube is given by [12]. Exemplarily the radial stress distribution for both isotropic and anisotropic materials is shown in the Figs. 3.13 and 3.14.

$$\sigma_r = p\left[\frac{c^{k+1}}{1-c^{2k}}(\rho^{k-1} - \rho^{-(k+1)})\right], \sigma_\theta = p\left[\frac{kc^{k+1}}{1-c^{2k}}(\rho^{k-1} + \rho^{-(k+1)})\right] \qquad [3.5]$$

where

$$\rho = \frac{r}{r_0}, c = \frac{r_i}{r_0}, k = \sqrt{\frac{\beta_{11}}{\beta_{22}}}$$

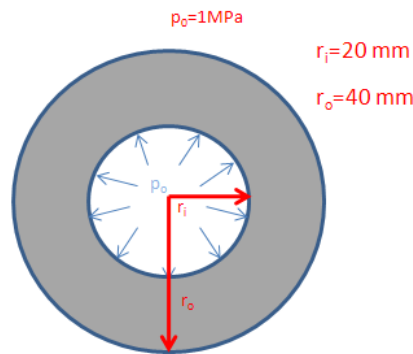$$\beta_{ij} = S_{ij} - \frac{S_{i3}S_{j3}}{S_{33}}$$

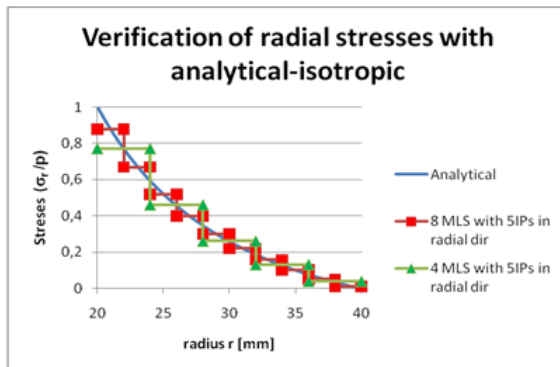Fig. 3.12: Problem description for thick walled cylinder internal pressure

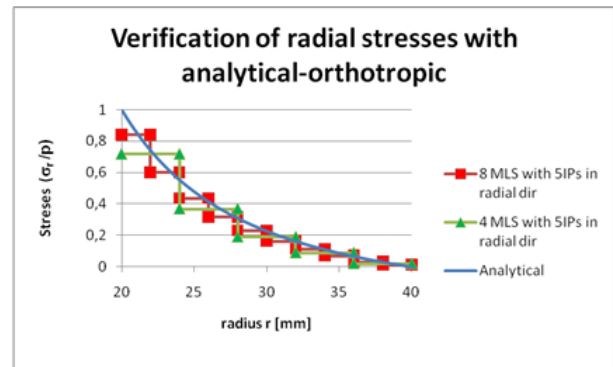Fig. 3.13: Distribution of radial stresses for isotropic case

Fig.3.14: Distribution of radial stresses for anisotropic case

3.5 Plate under uniform load

In this example, a simply-supported square cross-ply laminated plate (Fig. 3.15) is subjected to a uniform pressure p_o and the center deflection δ (Z-direction) of the plate due to the pressure load is determined. The stacking sequence of the plies is symmetric about the center plane. This problem has been verified from the reference [4, 10]. Also, the same problem has been simulated with layered elements from ANSYS [10]. The LS-DYNA layered solid element is in good agreement with the expected results (Table 3.3)
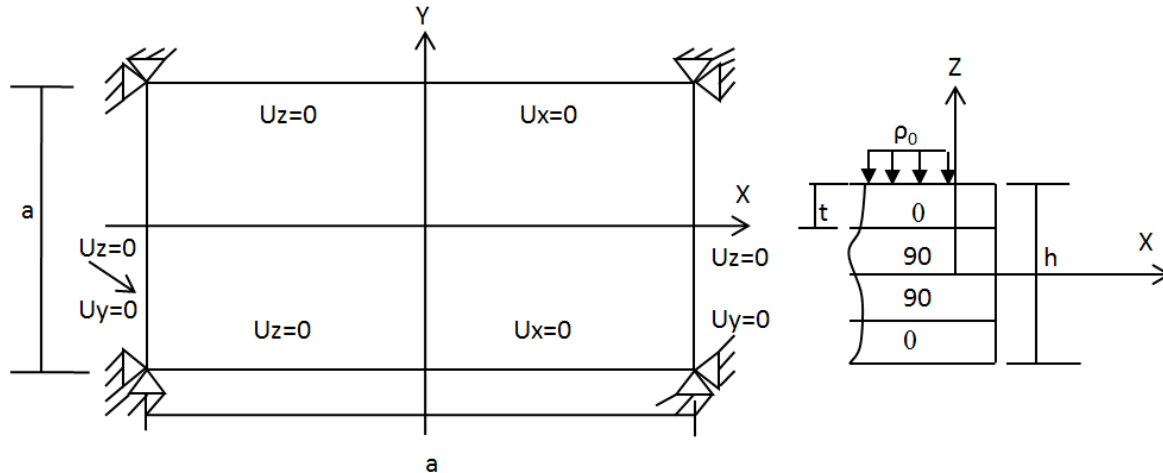
Fig. 3.15: Problem description for plate under uniform pressure loading [10]

Orthotropic material parameters for the above test are $E_{11} = 25 \times 10^6$ N/m^2, $E_{22} = E_{33} = 1 \times 10^6$ N/m2, $v_{21} = v_{31} = 0.028$, $v_{23} = 0.776$, $G_{12} = G_{13} = 0.5 \times 10^6$ N/m^2, $G_{23} = 0.2 \times 10^6$ N/m^2.

element type	target value for center deflection `w´ according to [4]	obtained value
ANSYS layered solid 46	0.0683	0.0676
ANSYS layered solid 185	0.0683	0.0676
ANSYS layered shell 181	0.0683	0.0681
LS-DYNA layered solid (tshell type5)	0.0683	0.0659

Table 3.3: Comparison of results with various layered elements

3.6 Pinched cylinder

This problem is a severe benchmark test for checking shear locking in thin shell structures. Fig. 3.16 shows a pinched cylinder subjected to a pair of concentrated loads, both ends of the cylinder are assumed to be free [5]. The parameters for the above test are $E = 105 \times 10^5$ lb/in^2, $v = 0.3125$, $L = 10.35$ in, $R = 4.95$ in, $t = 0.094$ in, $P = 100$ lb.
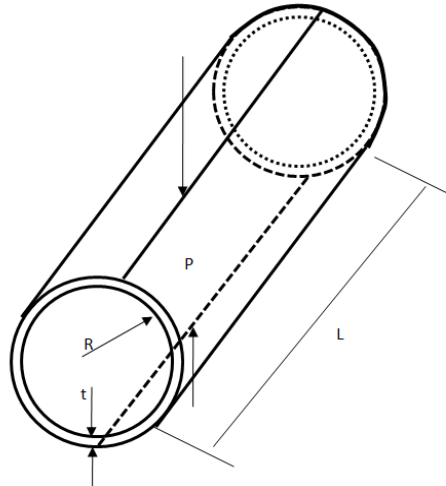
Fig.3.16. Pinched cylinder with dimensions [5]

The problem is simulated with standard type 2 shell element in LS-DYNA [11] and with the new multi-layered solid. The analytical solution for displacement at the loading point of pinched cylinder was computed as $w_{max} = 0.1137$ in.

Analytical solution (w_{max})	0.1137 in
Shell Type 2 with mesh density (20x20x1)	0.118 in
Multi-layered solid solution with mesh density (20x20x1)	0.116 in

Table 3.4: Displacement at loading point of pinched cylinder

Above table (Table 3.4) shows that shear locking can be avoided by the multi-layered solid element and could be used for thin shell applications as it has bending stiffness accuracy of a thin shell.

4   Component test with H_2 vessel

4.1 Test setup and component

To verify stability, required CPU time as well as pre- and postprocessor handlings of the new multi-layered solid element, simulations with H_2 vessel are performed. Cylindrical segments which are cut out of H_2 vessels are impacted, the intrusion of the impactor and the contact force are measured. Fig. 4.1 shows the basic setup of the test. The test conditions are chosen to perform 'test to failure' and do not represent loads which are measured in vehicle crash simulations.
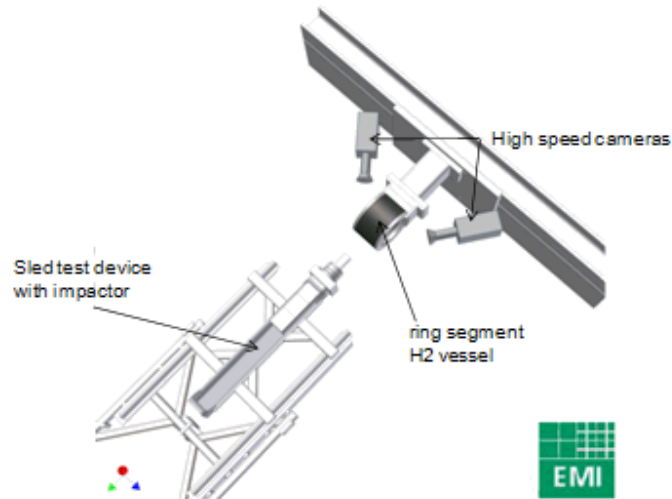
Fig. 4.1: Test setup H$_2$ vessel segment impact picture by courtesy of Ernst-Mach-Institut, Freiburg

4.2 LS-DYNA model

The test – see Fig. 4.1 – is analyzed with the finite element method. The measured data are compared to- results of three different models, which are explained below.

4.2.1 Multi-layered solid (TSHELL type 5) model

The LS-DYNA version 971_d_R4.2 used for the following simulation results allows the use of the new multi-layered solid element with material 22, *MAT_COMPOSITE_DAMAGE. Delamination is represented with *CONTACT-AUTOMATIC-SURFACE-TO-SURFACE-TIEBREAK contact. More than 100 plies of carbon fiber are represented with 5 multi-layered solid (TSHELL type 5) elements through thickness of the vessel. Every fiber orientation is stated in the *SECTION_TSHELL card. Therefore the option ICOMP (flag for layered composite material mode) must be set to 1 and an integration rule describing the relative thickness is required. Alternatively *PART_COMPOSITE card could be used.
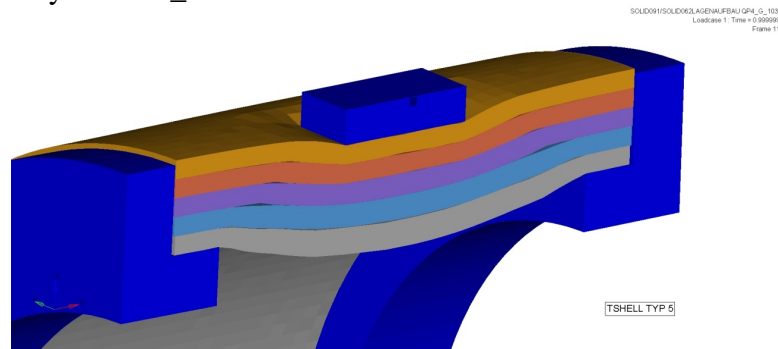

Fig. 4.2: Test setup of impact on H$_2$ vessel segment, modeled with multi-layered solid elements (TSHELL elform5)

4.2.2 One solid per ply model

This model uses default solid elements (type 1) with one integration point per ply. Ply direction for more than 100 plies is represented with the use of the AOPT option. Every fiber direction requires its own material card with an applicable orientation vector.
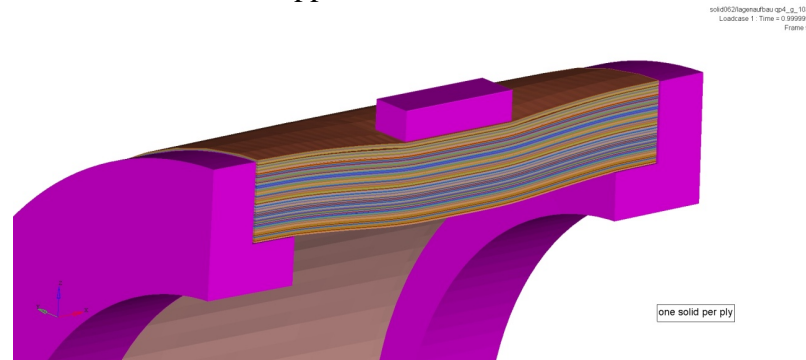

Fig. 4.3: Test setup of impact on H$_2$ vessel segment, modeled with one solid element for each ply

4.2.3 Model with engineering constants

This model uses 'smeared' (homogenized) stiffness properties calculated with the classical laminate theory. More than 100 plies of carbon fiber are represented with 5 default solid elements (type 1) through thickness of the vessel.

4.3 Simulation results

All three models can detect the onset of failure for the H$_2$ vessel in a crash event. Failure due to delamination is modeled with the *CONTACT-AUTOMATIC-SURFACE-TO-SURFACE-TIEBREAK. The authors have not encountered numerical instabilities. Table 4.1 shows the number of elements and the necessary CPU time for three FE-models, namely for one solid per ply, for the layered solids with several plies per element and for the one with homogenized stiffness properties.

model type	# elements	CPU time [h] of Win XP with 3 CPUs
one solid per ply	1.9 Mio	81.5
layered solid (tshell elform 5)	35,000	13.5
engineering constants	35,000	5

Table 4.1: Comparison of simulation models

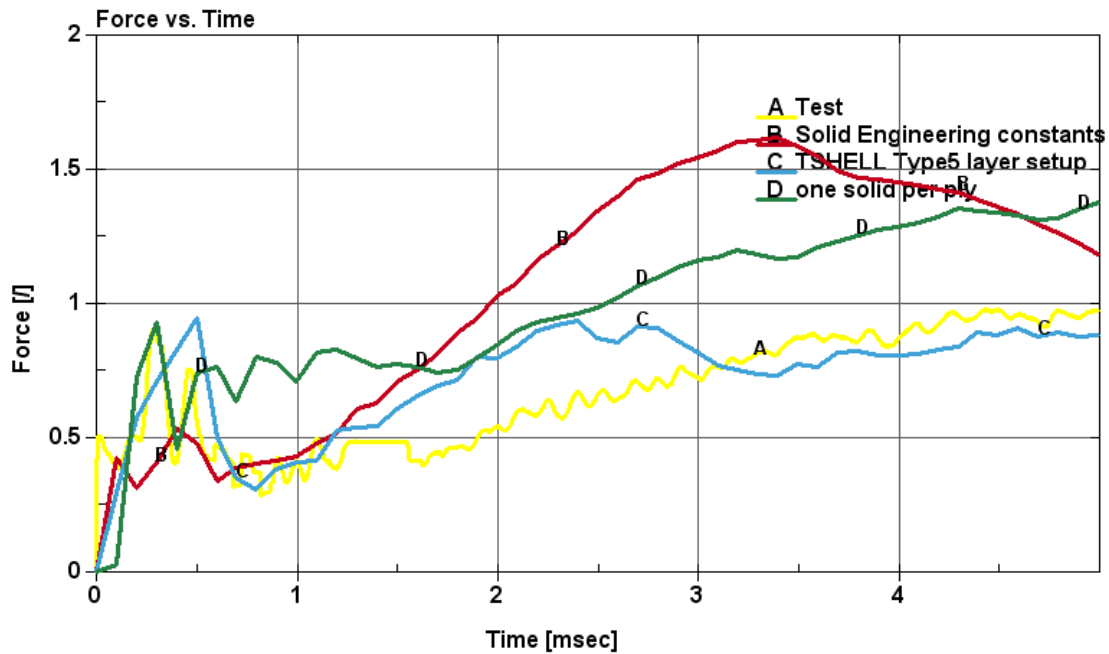Fig. 4.4 shows the force on the impactor with respect to time.

Fig.4.4: Result H_2 vessel segment impact → measured force over time with different element types

The intrusion history diagram of the impactor into the ring segment of the H_2 vessel is shown in Fig. 4.5. The force and intrusion results shown below in Fig.4.4 and Fig.4.5 are normalized.
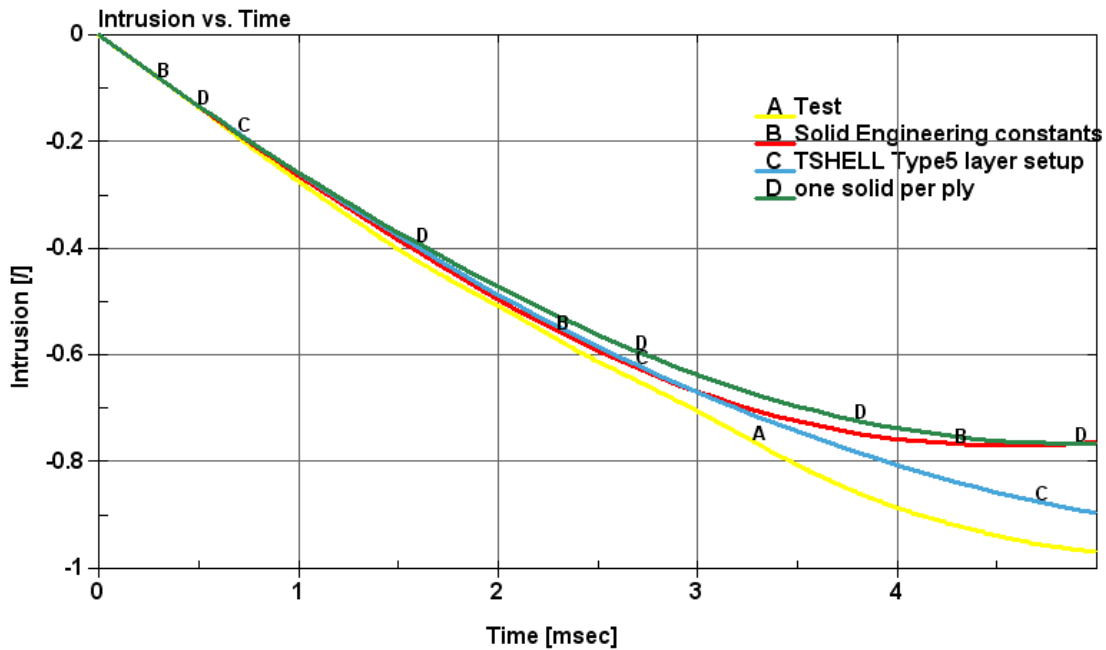

Fig.4.5: Result H_2 vessel segment impact→measured intrusion over time with different element types

5 Summary

The use of multi-layered solid (TSHELL elform=5) element offers a possibility to model thick composite lay-ups in detail with acceptable CPU times as well as an acceptable model size. One can take individual fiber orientations and ply thickness into account without the need to live with 'smeared' material properties. Multi-layered solid element which has multiple integration points through its thickness could be used for thin shell applications as it has bending stiffness accuracy of a thin shell. This element has several advantages like computing thickness stresses, and it is also important for certain problems where through the thickness deformations and strains are significant. The new multi-layered solid element (TSHELL elform = 5) should not be used with the one-point integration like the standard hexahedron in explicit analysis. Instead it is better to use standard hexahedron element.

6 References

[1]   Belytschko, T. and Bindeman, L.P.: Assumed strain stabilization of the eight-node hexahedral element. Computer Methods in Applied Mechanics and Engineering 1993; 105:225-260

[2]   Robbins, D.H. and Reddy, J.N.: Modeling of thick composites using a layerwise laminate theory. International Journal for Numerical Methods in Engineering 1993; 36:655-677

[3]   Fiolka, M. and Matzenmiller, A.: On the resolution of transverse stresses in solid shells with a multi-layer formulation. Communications in Numerical Methods in Engineering 2007; 23:313–326

[4]   Reddy, J.N.: Exact solutions of moderately thick laminated shells. ASCE Journal Engineering mechanics 1972; 110:5-805

[5]   Guo, Y.: Eight node solid element for thick shell simulations. 6th International LS-DYNA conference, Detroit, 2000

[6]   Valentin, S. and Stephan, F. et al: The hierarchical building-block approach of testing and FE analysis for strength prediction of high-pressure wet-wound composite vessels. SIMVEC VDI- Tagung, 2008

[7]   Eriq, Q.S.: Shear locking and hourglassing in MSC Nastran, ABAQUS and ANSYS. MSC Software Users Meeting, 2006

[8]   Werner, W.: Simulation and FE modeling of global and local effects in thin-walled shell structures of composite materials. NAFEMS Seminar on Simulating Composite Materials and Structures, Bad Kissingen, 2007

[9]   Nguyen, D.Q. and Matzenmiller, A.: A solid shell element with enhanced assumed strains for higher order shear deformations in laminates. Technische Mechanik, Band 28, Heft 3-4, S. 334-355, 2008

[10] ANSYS verification manual, ANSYS Inc., Pittsburg, 2009

[11] Hallquist, J.O.: LS-DYNA Theoretical Manual. Livermore Software Technology Corporation, Livermore, 2006

[12] Lekhnitskii, S.: Theory of elasticity of an anisotropic body, Mir Publisher, Moscow, 1981 (English translation)

Appendix

```
*PART_COMPOSITE_TSHELL
$#   pid   elform   shrf   nloc   marea   hgid   adpopt
      2        5   0.833      0       0      2        0
$ 4 Layers GFRP [45/-45/-45/45] each 0.008 mm thick
$   mid  thick ti   beta         mid  thick ti   beta
     1   0.008    45.0            1   0.008    -45.0
$   mid  thick ti   beta         mid  thick ti   beta
     2   0.008   -45.0            1   0.008    45.0
*CONTROL_SHELL
$#  wrpang    esort   irnxx   istupd   theory    bwc    miter    proj
  20.000000       0      -1        0        2      2        1
$# rotascl   intgrd   lamsht   cstyp6   tshell   nfail1   nfail4   psnfail
  1.000000       0        4        1
```